Доклади на Българската академия на науките
Comptes rendus de l'Académie bulgare des Sciences
Tome 78, No 3, 2025

SPACE SCIENCES
Space physics

IONOSPHERIC DISTURBANCES DURING STRONG GEOMAGNETIC STORM ST. PATRICK ON 17 MARCH 2015

Rumiana Bojilova[1]✉, Plamen Mukhtarov[1], Petra Koucká Knižová[2], Katya Georgieva[3], Boian Kirov[3]

Received on February 12, 2025
Presented by P. Velinov, Corresponding Member of BAS, on February 25, 2025

Abstract

In this paper, we examine both the global and local distribution of the ionospheric response represented by Total Electron Content (TEC) for a geomagnetic storm that occurred on 17 March 2015. The behaviour of the measured TEC and median TEC data was compared to analyze in detail the recorded ionospheric disturbance. Selected energy flux data show an increase in particle precipitation in the polar latitudes of both hemispheres, which are strongest in the midnight longitudinal sector. The results of the spatial distribution of TEC response as well as the behaviour of the ionosphere at individual points show that i) in the analysis of the Northern Hemisphere as a result of the additional ionization from particle precipitation in the night hours a positive ionospheric response is observed; ii) in the region of the polar oval in both hemispheres, the dependence of the response on local time illustrates the change of the predominant mechanism of the ionospheric response; and iii) spatial distributions of median TEC and measured TEC allow for a detailed analysis of the observed effects of Equatorial Ionization Anomaly (EIA), associated with the positive anomalies observed in TEC in the equatorial region.

Key words: geomagnetic storm, ionosphere, TEC

This work was partly supported by the Bulgarian National Science Fund grant KP-06-N44/2/27/11-2020 "Space weather over a period of the century solar activity descending", and the bilateral project No IC-CZ/04-2023-2024 between the Bulgarian Academy of Sciences and the Czech Academy of Sciences "Solar influences on the interactions in the atmosphere-ionosphere system". This work was partly supported by the Bulgarian Ministry of Education and Science under the National Research Programme "Young scientists and postdoctoral students-2" approved by DCM 206/07.04.2022.

https://doi.org/10.7546/CRABS.2025.03.10

Introduction. It is well known that the so-called geomagnetic storms are some of the most important events for solar-terrestrial physics due to their impact on the positioning accuracy of GNSS receivers, radio communication, and in some rare cases even disruption of power grids [1]. As a result of the interaction between the solar wind and the magnetosphere-ionosphere system during geomagnetic storms, ionospheric disturbances occur which are manifested in terms of large deviations of ionospheric behaviour from the regular quiet time behaviour. The ionospheric density or electron content is found to be either enhanced (positive storm) or depleted (negative storm) depending on the local time of the storm commencement, season, latitude, and longitude of observation [2]. The positive ionospheric changes during the main phase of the geomagnetic storm are a result from changes in the equatorward winds, while the negative ionospheric response is a result of increases of molecular nitrogen [3]. The strongest geomagnetic storm of 24th Solar Cycle namely, the St. Patrick's geomagnetic storm recorded on 17 March 2015 has been well studied by scientists working in the field of space physics and solar-terrestrial physics [1, 4–8]. The effects on the ionospheric response resulting from this storm, observed at mid and low-latitude, are related to two of the main physical processes: (i) the prompt penetration of magnetospheric convection electric field (PPEF), and (ii) the dynamo effects of the storm winds disturbance dynamo electric field (DDEF). The main purpose of this study is to examine the ionospheric anomalies during St. Patrick geomagnetic storm in March 2015 by comparing the variations in the measured, median and relative values of TEC on a global and regional scale.

Data. As already mentioned, for the purposes of ionospheric studies it is of great importance to trace and analyze the behaviour of the electron density in disturbed conditions caused by the interaction of charged particles from the Sun and the Earth's magnetosphere. To study the behaviour of the ionosphere under the influence of geomagnetic disturbances, several basic parameters were used, characterizing the behaviour of the geomagnetic storm as well as the phases of its development. In this study, the indices Kp and Dst received from Goddard Space Flight Center were used (`https://omniweb.gsfc.nasa.gov/`). Another parameter used to determine the amount of particle precipitation in the auroral region is obtained from the OVATION Prime Real-Time model and provides information about energy flux [9]. All of these parameters indicate disturbed conditions, which is a possible indication of ionospheric anomalies. This type of ionospheric disturbances have been analyzed based on data for TEC by the Center for Orbit Determination in Europe (CODE) which are provided by `ftp://ftp.unibe.ch/aiub/CODE/`. It is accepted that daily and seasonal variability of ionospheric quantities and their dependence on long-term changes in solar activity are given by the monthly median of hourly values. The advantage of using the median value over the average one is due to the elimination of the influence of several extreme values recorded during geomagnetic disturbances [10].

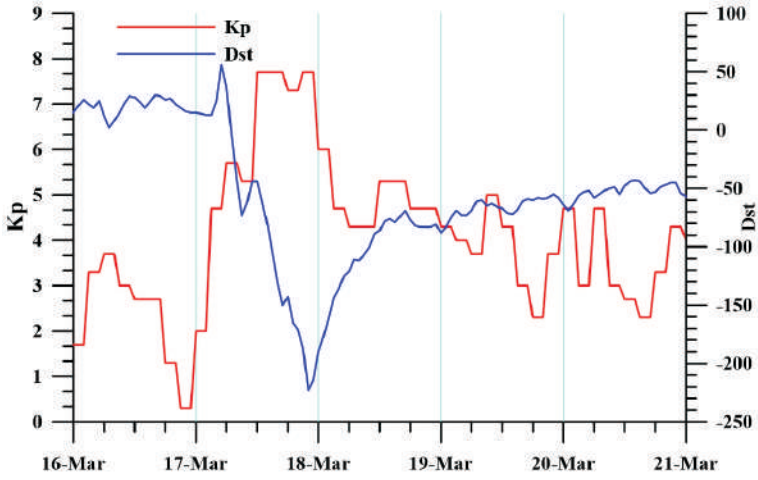

Fig. 1. Geomagnetic indices Kp and Dst for the period 16–21 March 2015

Traditionally to characterize the quiet geomagnetic conditions at selected month the medians are used [11]. Anomalies in electron density are estimated by introducing the quantity relative deviation. This characteristic allows to determine with sufficient accuracy the type of ionospheric response (positive or negative) in each specific case [12].

Geomagnetic conditions. In order to assess the variations of the geomagnetic field caused by the interaction of charged particles from the Sun and the Earth's magnetosphere, the two indices Dst and Kp have been selected. The presented behaviour of the Dst index (blue colour) in Fig. 1 shows that in the hours after 6 UT on 17 March (the beginning of the storm) the index starts to decrease, reaching a minimum value of around –220 [nT] around 22 UT on 17 March (the maximum of the storm). According to the accepted classifications for the Dst index, this storm is of the intense storm type [13]. It gives the impression that during the entire period 18–20 March, Dst index remains relatively high (around –50 nT), which corresponds to disturbed geomagnetic conditions. The other parameter, namely the Kp index, shown in Fig. 1 (red colour) illustrates a similar manifestation of the geomagnetic storm analogous to that of the Dst index. In the hours around 6 UT on 17 March, the Kp index shows values above 5, which is an indicator of a disturbance. The maximum value of Kp is in the hours between 12 UT-23 UT on 17 March, reaching $7\frac{2}{3}$. The recovery phase lasts several days. According to the accepted classification of the National Oceanic and Atmospheric Administration (NOAA), the studied geomagnetic storm is G3 Strong (`https://www.swpc.noaa.gov/noaa-scales-explanation`).

Behaviour of Power Index. To represent the influence of particle precipitation for the Northern Hemisphere and Southern Hemisphere, as well as the

total Energy Flux, data from the OVATION Prime model, whose data are derived from electron and proton flux measurements from the SSJ4 detectors on the DMSP satellites, as well as OVATION Prime-2013-nowcast data, were used [14,15]. From the sum of the energies for both hemispheres shown in Fig. 2 (upper panel) it can be seen that the beginning of the geomagnetic storm can be determined at 06 UT 17.03.2015 when the Power Index (PI) sharply increases. A possible explanation for the observed phenomenon is given by Kamide and Kusano [16], who suggest that "an intense storm can result from the superposition of two successive, moderate storms, driven by two successive, southward IMF structures". Similarly to the geomagnetic indices, the Power Index for the entire period also remains higher as compared to before the geomagnetic storm. This result suggests that it is possible that energy flows will continue to flow into the Polar Regions during the entire period 18–20 March.

The bottom panels of Fig. 2 present the latitudinal dependence of energy flux entering into both hemispheres at two selected longitudes. The results from the graph show that during the period 18–20 March there is particle precipitation in the polar latitudes of both hemispheres, which are strongest in the midnight longitudinal sector. This fact confirms that the recovery phase of the geomagnetic storm does not occur under quiet conditions. In the Southern Hemisphere, the positive response associated with the particle precipitation into the polar oval has

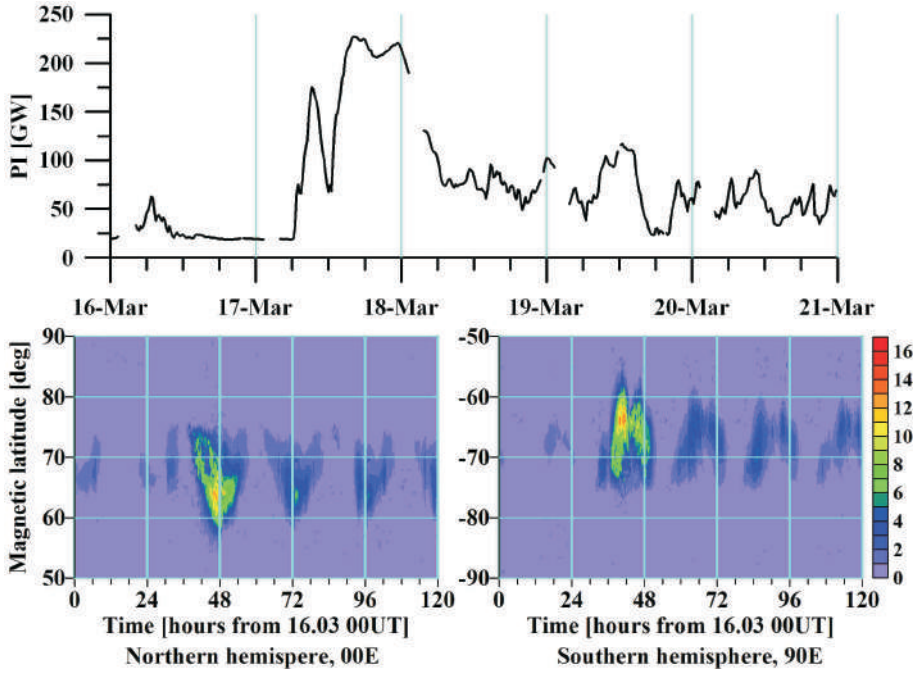

Fig. 2. Earth Power Index OVATION Prime-2013 nowcast – upper panel and OVATION Prime Real-Time model, energy measured at flux in ergs/(cm^2/s) bottom panel

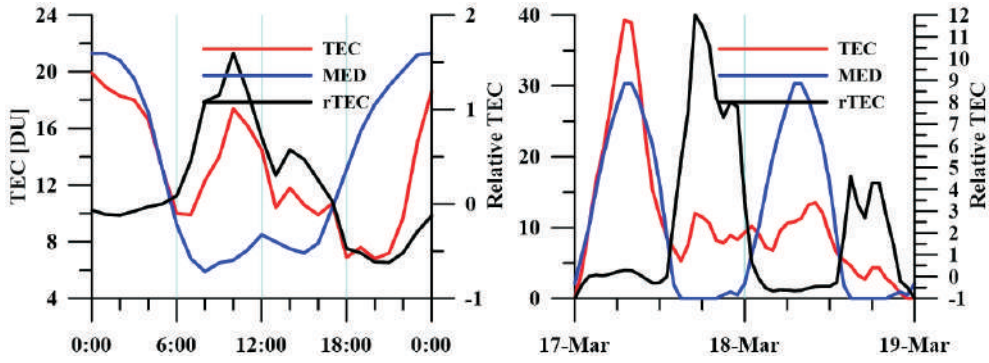

Fig. 3. Comparison between measured TEC (red colour), relative TEC (black colour) and median TEC (blue colour) on 17 March at point with coordinates 60°N, 210°E – left panel. Analogous to the left panel, but at point with coordinates 45°S, 90°E and for the period 17–18 March – right panel

a more complex character due to the strong deformation of the Earth's magnetic field.

Ionospheric response. In order to study in detail the influence of particle precipitation in auroral region in both hemispheres on the electron density, the ionospheric response for the period 17–18 March is presented at two selected points corresponding to the most significant positive anomalies in the Power Index. Figure 3, left panel, illustrates a comparison between the measured TEC, the median TEC (MED) and the relative deviation of the TEC (rTEC) for the point located in the Northern Hemisphere with coordinates 60°N, 210°E on 17 March. Figure 3, right panel is analogous to the left part of Fig. 3 and presents a comparison of the behaviour of the three characteristics, but for a point in the Southern Hemisphere with coordinates 45°S, 90°E and for the period 17–18 March. The left part of Fig. 3 shows an increase of rTEC and TEC in the hours after 6 UT on 17 March, which indicates the beginning of the ionospheric anomaly because of the geomagnetic storm that occurred.

The results presented in Fig. 3, right panel show that at the point with coordinates 60°N, 210°E, the additional ionization occurs in the nighttime hours and its maximum is at about 10 UT. This coincides with midnight local time, after which the TEC decreases even though the Power Index increases, which is due to the shift of the midnight zone. After the onset of the day, a negative ionospheric response has already been observed, due to the predominance of the mechanism of increased recombination due to the heating of the neutral air.

Figure 4 shows the spatial distributions of median TEC (left column panels) and measured TEC (right column panels) for the final phase of the storm (from 18 UT to 00 UT on 17–18 March). Figure 4 (right column) shows that at 18 UT, a visible expansion of the Equatorial Ionization Anomaly (EIA) especially in the longitudes between 30°W and 30°E, as well as a shift of the northern maxi-

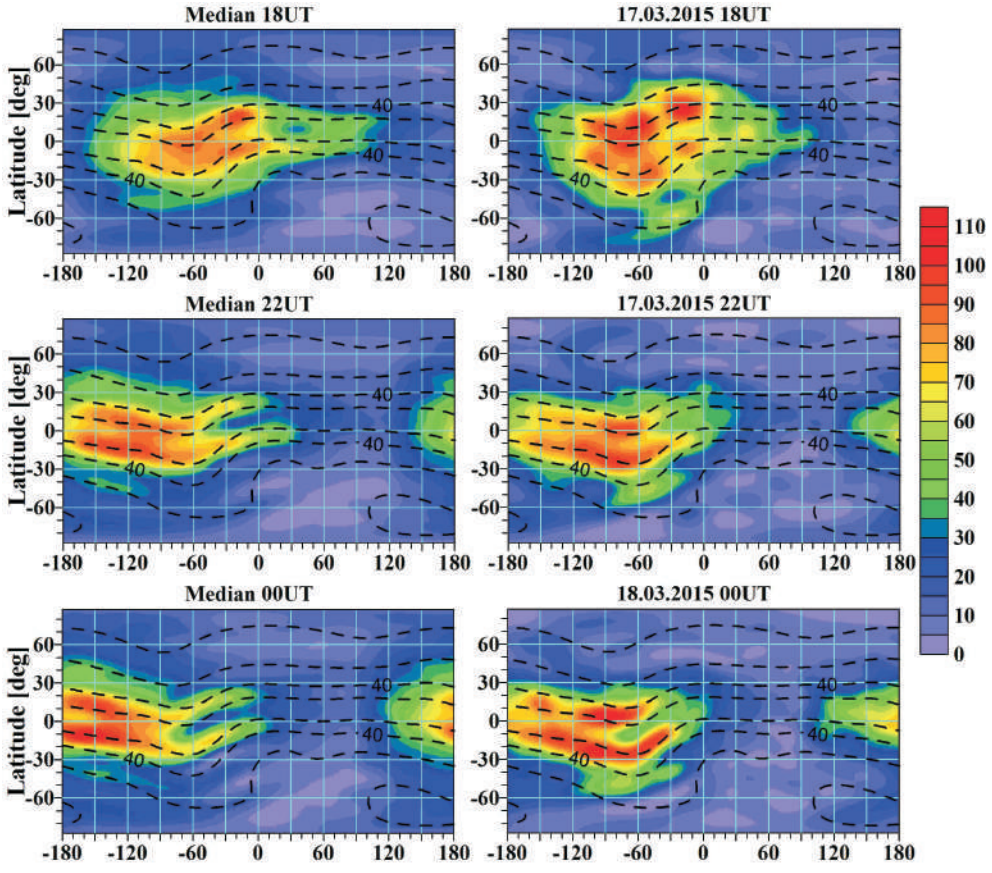

Fig. 4. Spatial distribution of: a) left column panels – median TEC, and b) right column panels – measured TEC at 18 UT and 22 UT on 17 March and 00 UT on 18 March

mum in the north direction is observed. The observed increases at low latitudes are localized in the afternoon and evening hours and characterized the poleward movement of the enhanced equatorial crests. The presented maps at 22 UT and 00 UT show an increase but no apparent EIA expansion. The expansion of the EIA can be explained by the effects of the "perturbed dynamo" in the equatorial region, which affects the "fountain effect" and which manifests itself with a certain delay necessary to reach the equator of the anomalous meridional wind, which, due to Coriolis acceleration, passes into the zonal [17, 18].

Conclusion. This study presents the global and regional distribution of electron density anomalies resulting from the geomagnetic storm that occurred on 17 March 2015 [19, 20]. For the purposes of this work, comparisons are shown between the measured, median values and relative deviation of the TEC for two selected points from each hemisphere, for which a maximum value of the incoming radiation from the Sun, measured by the Power Index, was obtained. The results

of this comparison for the point in the Northern Hemisphere with coordinates 60°N, 210°E show an increase of rTEC and TEC in the hours after 6 UT on 17 March – which corresponds to the ionospheric response as a result of the recorded geomagnetic storm. The other point, located in the Southern Hemisphere with coordinates 60°N, 210°E, shows that the additional ionization occurs in the night-time hours. In local time, the maximum at this point coincides with midnight, after this moment the TEC decreases, which is due to the shift of the midnight zone.

Another key result of the present analysis is related to the comparison between the spatial distribution of median TEC and measured TEC for the period 18 UT on 17 March to 00 UT on 18 March. The presented spatial maps trace the evolution of the EIA phenomenon and its effect on ionospheric variations at low and mid latitudes. In the hours around 18 UT, the TEC values show an extension of the EIA effect, reaching mid-latitudes, especially in the longitudes between 30°W and 30°E. The presented maps at night hours show an increase in TEC, but without the presence of an EIA extension. The observed increases at low latitudes are localized in the afternoon and evening hours.

REFERENCES

[1] Wu C. C., K. Liou, R. P. Lepping et al. (2016) The first super geomagnetic storm of solar cycle 24: "The St. Patrick's day event (17 March 2015)", Earth Planets Space, **68**, 151, 1–12.

[2] Field P. R., H. Rishbeth (1997) The response of the ionospheric F2-layer to geomagnetic activity: an analysis of worldwide data, J. Atmos. Solar-Terr. Phys., **59**(2), 163–180.

[3] Fuller-Rowell T. J., M. V. Codrescu, R. J. Moffett, S. Quegan (1994) Response of the thermosphere and ionosphere to geomagnetic storms, J. Geophys. Res: Space Physics, **99**(A3), 3893–3914.

[4] Nayak C., L. C. Tsai, S. Y. Su et al. (2016) Peculiar features of the low-latitude and midlatitude ionospheric response to the St. Patrick's Day geomagnetic storm of 17 March 2015, J. Geophys. Res: Space Physics, **121**(8), 7941–7960.

[5] Nava B., J. Rodríguez-Zuluaga, K. Alazo-Cuartas et al. (2016) Middle- and low-latitude ionosphere response to 2015 St. Patrick's Day geomagnetic storm, J. Geophys. Res: Space Physics, **121**(4), 3421–3438.

[6] Astafyeva E., I. Zakharenkova, M. Förster (2015) Ionospheric response to the 2015 St. Patrick's Day storm: A global multi-instrumental overview, J. Geophys. Res: Space Physics, **120**(10), 9023–9037.

[7] Sripathi R. S., S. Sreekumar, S. Banola et al. (2015) Low-latitude ionosphere response to super geomagnetic storm of 17/18 March 2015: Results from a chain of ground-based observations over Indian sector, J. Geophys. Res: Space Physics, **120**(12), 10864–10882.

[8] Huang C. S., G. R. Wilson, M. R. Hairston et al. (2016) Equatorial ionospheric

plasma drifts and O+ concentration enhancements associated with disturbance dynamo during the 2015 St. Patrick's Day magnetic storm, J. Geophys. Res: Space Physics, **121**(8), 7961–7973.

[9] Newell P. T., K. Liou, Y. Zhang et al. (2014) OVATION Prime-2013: Extension of auroral precipitation model to higher disturbance levels, Space Weather, **12**(6), 368–379.

[10] Bojilova R., P. Mukhtarov (2023) Comparative Analysis of Global and Regional Ionospheric Responses during Two Geomagnetic Storms on 3 and 4 February 2022, Remote Sensing, **15**(7), 1739, https://doi.org/10.3390/rs15071739.

[11] Bojilova R., P. Mukhtarov (2023) Analysis of the Ionospheric Response to Sudden Stratospheric Warming and Geomagnetic Forcing over Europe during February and March 2023, Universe, **9**(8), 351, https://doi.org/10.3390/universe9080351.

[12] Danilov A. D., J. Lastovicka (2001) Effects of geomagnetic storms on the ionosphere and atmosphere, Int. J. Geomagn. Aeron., **2**(3), 209–224.

[13] Temerin M., X. Li (2015) The Dst index underestimates the solar cycle variation of geomagnetic activity, J. Geophys. Res: Space Physics, **120**(7), 5603–5607.

[14] Newell P. T., T. Sotirelis, S. Wing (2009) Diffuse, monoenergetic, and broadband aurora: The global precipitation budget, J. Geophys. Res: Space Physics, **114**(A9), 1–20.

[15] Machol J. L., J. C. Green, R. J. Redmon et al. (2012) Evaluation of OVATION Prime as a forecast model for visible aurorae, Space Weather, **10**(3), 1–8.

[16] Kamide Y., K. Kusano (2015) No major solar flares but the largest geomagnetic storm in the present solar cycle, Space Weather, **13**(6), 365–367.

[17] Richmond A. D. (1979) Ionospheric Wind Dynamo Theory: A Review, J. Geomag. Geoelec., **31**(3), 287–310.

[18] Yamazaki Y., M. J. Kosch (2015) The equatorial electrojet during geomagnetic storms and substorms, J. Geophys. Res: Space Physics, **120**(3), 2276–2287.

[19] Velinov P. I. Y. (1968) On ionization of the ionospheric D-region by galactic and solar cosmic rays, J. Atmos. Terr. Phys., **30**(11), 1891–1905.

[20] Potužníková K., P. Koucká Knížová, J. Chum et al. (2023) Summer tropospheric mesoscale situations with impact on the ionospheric plasma, Solar Influences on the Magnetosphere, Ionosphere and Atmosphere, 89–95.

[1] *National Institute of Geophysics, Geodesy and Geography, Bulgarian Academy of Sciences, Akad. G. Bonchev St, Bl. 3, 1113 Sofia, Bulgaria*
e-mails: rbojilova@geophys.bas.bg, engpjm@abv.bg

[2] *Institute of Atmospheric Physics, Czech Academy of Sciences, Bocni II 1401, 141 31 Prague, Czech Republic*
e-mail: pkn@ufa.cas.cz

[3] *Space Research and Technology Institute, Bulgarian Academy of Sciences, Akad. G. Bonchev St, Bl. 1, 1113 Sofia, Bulgaria*
e-mails: KGeorgieva@space.bas.bg, bkirov@space.bas.bg